AD-A178 453 FUNDAMENTAL STUDIES IN THE MOLECULAR BASIS OF LASER INDUCED RETINAL DAMAGE(U) CORNELL UNIV ITHACA N Y DEPT OF APPLIED PHYSICS A LEWIS 31 DEC 86 DAMD17-85-C-5136 1/1

UNCLASSIFIED F/G 6/18 NL

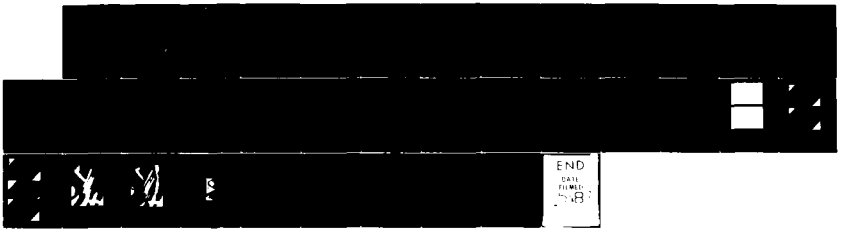

END
DATE
FILMED
3-87
DTIC

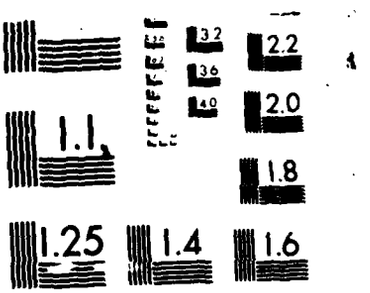

AD _____

FUNDAMENTAL STUDIES IN THE MOLECULAR BASIS OF LASER INDUCED RETINAL DAMAGE

ANNUAL REPORT

AARON LEWIS

DECEMBER 31, 1986

Supported by

U.S. ARMY MEDICAL RESEARCH AND DEVELOPMENT COMMAND
Fort Detrick, Frederick, Maryland 21701-5012

85 5136

Contract No. DAMD17-[redacted]-C-[redacted]

Department of Applied Physics
Cornell University
Ithaca, New York 14853

Approved for public release; distribution unlimited

The findings in this report are not to be construed as an official Department of the Army position unless so designated by other authorized documents.

SECURITY CLASSIFICATION OF THIS PAGE AD-A178453

REPORT DOCUMENTATION PAGE

Form Approved OMB No. 0704-0188

1a. REPORT SECURITY CLASSIFICATION UNCLASSIFIED	1b. RESTRICTIVE MARKINGS
2a. SECURITY CLASSIFICATION AUTHORITY	3. DISTRIBUTION/AVAILABILITY OF REPORT Approved for public release; distribution unlimited
2b. DECLASSIFICATION/DOWNGRADING SCHEDULE	
4. PERFORMING ORGANIZATION REPORT NUMBER(S)	5. MONITORING ORGANIZATION REPORT NUMBER(S)
6a. NAME OF PERFORMING ORGANIZATION Department of Applied Physics Cornell University 6b. OFFICE SYMBOL (If applicable)	7a. NAME OF MONITORING ORGANIZATION
6c. ADDRESS (City, State, and ZIP Code) Ithaca, New York 14853	7b. ADDRESS (City, State, and ZIP Code)
8a. NAME OF FUNDING/SPONSORING ORGANIZATION U.S. Army Medical Research & Development Command 8b. OFFICE SYMBOL (If applicable) SGRD-RMI-S	9. PROCUREMENT INSTRUMENT IDENTIFICATION NUMBER DAMD17-[redacted]-C-[redacted] 85 5136
8c. ADDRESS (City, State, and ZIP Code) Fort Detrick Frederick, MD 21701-5012	10. SOURCE OF FUNDING NUMBERS PROGRAM ELEMENT NO. 62772A; PROJECT NO. 3E1-62772A878; TASK NO. BA; WORK UNIT ACCESSION NO. 210

11. TITLE (Include Security Classification)
(U) Fundamental Studies in the Molecular Basis of Laser Induced Retinal Damage

12. PERSONAL AUTHOR(S)
Lewis, Aaron

13a. TYPE OF REPORT	13b. TIME COVERED	14. DATE OF REPORT (Year, Month, Day)	15. PAGE COUNT
Annual	FROM 5/1/85 TO 4/30/86	1986 December 31	32

16. SUPPLEMENTARY NOTATION

17. COSATI CODES			18. SUBJECT TERMS (Continue on reverse if necessary and identify by block number)
FIELD	GROUP	SUB-GROUP	
20	05		
06	18		

19. ABSTRACT (Continue on reverse if necessary and identify by block number)

20. DISTRIBUTION/AVAILABILITY OF ABSTRACT ☐ UNCLASSIFIED/UNLIMITED ☒ SAME AS RPT. ☐ DTIC USERS	21. ABSTRACT SECURITY CLASSIFICATION UNCLASSIFIED
22a. NAME OF RESPONSIBLE INDIVIDUAL Mary Frances Bostian	22b. TELEPHONE (Include Area Code) 301/663-7325 22c. OFFICE SYMBOL SGRD-RMI-S

TABLE OF CONTENTS

are discussed

Over the past one and a half years of our contract (DAMD17-85-C-5136) we have seen extraordinary progress in numerous areas. These areas have included continuing progress on the fundamental effects of femtosecond laser pulses with retinal pigments, new insights into the detailed interactions of light with photo-receptor cells, and tremendous advances in new forms of super-resolution microscopy that we pioneered with help from the Letterman Army Institute of Research. In the following sections progress in each of the above areas will be reviewed.

Femtosecond Pulses and Retinal Pigments

is used

The past year has seen unique progress in our investigations of the effect of femtosecond pulses with retinal pigments. Specifically we have been able to apply a unique new method of investigating the effect of femtosecond pulses using nanosecond lasers that are common in most laser laboratories. The laser we have used for this new methodology is the common Nd:YAG laser pumping a dye laser. To understand the essence of this new approach it must be realized that the nanosecond pulses that are emitted from such a laser can be made to have a large frequency or energy spread. This corresponds to an ultrashort coherence time for the photons. In other words this new method does not create femtosecond pulses by building a complex femtosecond laser but by modulating the energy spread in conventional lasers to generate pulses with ultrashort coherence times. In the present work we demonstrate as will be seen below that such temporally long but broad-bandwidth laser pulses can indeed be employed to provide unambiguous information concerning relaxation processes occuring on time scales much shorter than the excitation pulse durations.

One of the methods that we have employed for obtaining such high temporal resolution using broad-bandwidth light involves the mixing in a special non-linear crystal of three beams that were split off from the original laser and sent through the sample. Two of the three beams are time-delayed one with respect to the other and as a function of this time-delay a fourth laser beam is generated by the electronic/non-linear properties of the sample at another frequency. Thus, as the sample is being changed by light on a femtosecond timescale, the fourth laser beam, that is produced by mixing the three beams in the sample, is being altered in its intensity and this is plotted out as a function of the displacement of the two laser beams described above. Retinal pigments have coherence dephasing rates that significantly exceed the population thermalization rates and calculations we have

completed show that for such systems broadband excitation provides the most clear-cut information on ultrafast relaxation processes.

During the past year we have not only been able to set up this system of ultrahigh-frequency interference we have also been able to compare our results using direct measurements with the femtosecond system we built on the previous contract. As outlined in the proposal that we wrote for the present contract improvements were planned in our femtosecond laser to produce a 30 fsec continuum and these improvements have been completed. Therefore, as described below, we are now in a position to compare the results using ultrahigh frequency interference with those obtained by using the direct methodology outlined in our previous proposal.

To test our systems, we first completed extensive experiments on laser dyes that have been the standards for testing picosecond and femtosecond systems. One of the first dyes tried was cresyl fast violet and the dephasing we measured with the femtosecond (direct) system and the ultrahigh frequency (indirect) system was 0.7 psec in both systems. However the margin of error was 0.2 psec with the direct system and only 0.02 psec or 20 rsec with the indirect method. The next experiments centered on the laser dye rhodamine 6G and the measurements with the direct and indirect methods were 40fsec with both methods but the error was 40fsec with the direct method and only 10fsec with the indirect method. Subsequently, we began investigations on pigments that were more relavent to retinal processes. For our initial experiments in this direction we investigated the dephasing differences between N-retinylidene Schiff bases (NRB) and N-retinylidene protonated Schiff bases (NRBH). The direct method was unable to detect any differences in the dephasing times between these two systems. However, the indirect method was able to show that depending on the position of the broadband dye laser the dephasing of the NRB system after light excitation was either 30fsec longer or shorter than the NRBH system. Specifically at 424nm the dephasing of NRB was shorter while at 546 nm the NRB system was longer. These differences in dephasing seems to be connected with whether the molecules are excited in the 0-0 transition or at energies that are higher than the 0-0. Experiments to confirm these suggestions are continuing.

With these test experiments completed we approached our first experiments with visual pigments with a great deal of confidence and we were not disappointed. The first results are presented in Figure 1. In this figure two separate experiments of the dephasing of mudpuppy cone rhodopsin are presented using

the indirect methodolgy. As can be seen, the 75fsec dephasing time is duplicated with an error of less than 3fsec. There were errors of at least 50fsec in the dephasing time as determined using the direct methodolgy.

In summary, these new methods of investigating femtosecond processes in retinal tissue gives us a new and important approach for understanding in detail the effects of femtosecond pulsed lasers on the retina. The availability of both these femtosecond systems and the unique environment at the Hadassah Hospital and Hebrew University will give us a new flexibility which will allow us to combine detailed physical measurements with first rate pathology in order to reach a new level of understanding on the effects of femtosecond laser pulses on retinal tissue.

II. Fundamental Interactions of Light with Photoreceptors

A. The Role of Mechanical Coupling in Visual Transduction

1. A guiding framework to design new experiments

Over the past two years we have begun to develop new ideas that govern our understanding of photoreceptors and how these cells respond to all forms of light from lasers to other light sources. As a result of research on our previous contract with the U.S. Army (#DAMD 17-79-C-9041) we were able to show that visual photoreceptors have a detailed filamentous structure that acts as a cytoskeleton. This cytoskeleton is elastic and connects, in rod cells, the discs to each other and to the plasma membrane. As a direct result of this study we began to ask if there was a need to be constrained by the hypotheses that governed, for several decades, our understanding of the interaction of light with these cells. The dominant hypothesis was based on the assumption that the discs are separate from one another and from the plasma membrane and thus, diffusable second messangers were required to transmit the cellular signals from photolyzed rhodopsin to the cellular plasma membrane. The principal facts that required such a hypothesis were the apparent physical (1) and electrical (2) isolation of the discs from the plasma membrane. However, the experimental evidence obtained under the previous contract with the Army and supporting data from other workers (3,4) has demonstrated that the presumed physical isolation of the discs is in fact not correct.

In view of the above and other evidence discussed below we developed alternate approaches to view amplification and adaptation in rod cells based on this experimentally observed cytoskeletal coupling (5,6). Our model accounts for many of the biochemical, electrophysiological, physical and cytological

results and demonstrates that there are other schemes, consistent with mechanisms in other cellular systems, that cna integrate the data presently available on amplification and sensitivity control. Our intention in developing this new perspective was to provide a framework for understanding and designing experiment aimed at further elucidating the molecular mechanism of visual transduction.

Any successful model for visual transduction must account for all of the known experimental facts. These experimental results can be grouped according to four catagories: cytological, physical, biochemical and electrophysiological.

(a) Cytological: In toad rod outer segments (ROS) there are 8000 filaments/disc or 1.6×10^7 filaments per cell. In addition to these axial filaments, there are multiple radial filaments connecting discs to the plasma membrane. The composition of these filaments is not known, but they appear to be highly plastic since they can be significantly stretched prior to breaking (3).

(b) Physical: Cytologically well-preserved whole ROS and stacks of ROS discs exhibit rapid (10-50 msec) anisotropic infrared light scattering changes in response to illumination (7). The physical basis of these light scattering changes is light-induced longtitudinal shrinkage with a decrease in lattice spacing along the rod outer segment (7). The maximum light-induced decrease in ROS length has been estimated to be 0.3-1% by infrared light scattering (7), neutron scattering (8), and x-ray diffraction (9).

(c) Biochemical: These light-induced changes in outer segment length are triggered by biochemical changes in ROS (7). Specifically, absorption of light by rhodopsin leads to binding of a protein, called transducin (T) or G. to the spectral intermediate metarhodopsin II. It has been shown that the physical result of T-protein binding is the ROS shrinkage described above. The biochemical result of the associaition of T-protein to rhodopsin is to initiate a sequence of reactions that activiates a phosphodiesterase (PDE), causing it to hydrolyze up to 4×10^5 cyclic GMP/sec-photon absorbed in vitro, it is not clear if this results in a precipitous reduction in cyclic GMP in vivo (11). A possible reason for the lack of unanimity in accepting a large cyclic GMP reduction in vivo is the recent demonstation that light also activiates a guanylate cyclase to synthesize cyclic GMP (12,13). This light-induced increase in cyclic GMP synthesis appears to occur over the same time course and same change in light intensity as the electrophysiological response (12,13). These observations support a hypothesis in

which light-induced acceleration of cyclic GMP hydrolysis and synthesis rather than simply a decrease in cytoplasmic cyclic GMP, may be an important factor in visual transduction.

An additional aspect of ROS biochemistry is that there is a light sensitive calcium pool and that light can alter this pool by up to $3x10^7$ calcium ions (14,15). These results have generally been interpreted as implicating intracellular binding sites for calcium, but experiments aimed at determining the location of these binding sites have been inconclusive (16). One possibility that would fit a mechanical transduction hypothesis and that has not been explored is that the light sensitive calcium pool in ROS may be associated with the $1.6x10^7$ disc-to-disc filaments/toad ROS observed by electron microscopy. If this is the case, then with light there would be an alteration in the binding of approximately 2 calciums/filament. Additional results indicate that alterations in the intracellular binding of calcium are regulated by cyclic GMP hydrolysis (17) and possibly inositol triphosphate (18).

(d) Electrophysiological: It is known that absorption of a single photon by a dark-adapted ROS decreases the dark current of 20 pa by 1 pa (19), and the amplitude of the electrical response adapts over several log units of background light intensity (20). Excitation and adaptation are highly localized with ROS, spreading less than 8 microns from the site of photon absorption (21). The membrane Na conductance is non-selective, as it is permeable to K, Li, Rb, Cs, Sr, and Ba (22). Each membrane channel carries a current of 3 fa (23,24) implying that approximately 350 channels must be closed by a single photon. Cyclic GMP binds directly to the membrane channel and decreases the permeability of this channel to Na ions (23,24).

The observation that cyclic GMP closes membrane sodium channels and that ROS contain a light activated PDE highly specific to cyclic GMP has been interpreted to suggest that cyclic GMP hydrolysis is responsible for initiating visual excitation (23,24,25). However, it is not unanimously accepted that light causes a large and rapid reduction in cyclic GMP in vivo and this could be due to light-induced guanylate cyclase activity described above. These observations may support a model in which a light-induced increase in cyclic GMP hydrolysis and synthesis, rather than a decrease in cyclic GMP, plays an important role in visual transduction. In addition, models in which light-activated PDE directly attacks the cyclic GMP molecules bound to the channels are excluded because of the diffusion times involved for large molecules such as PDE moving from the disc where they are excited to the plasma membrane. Finally, the growing list of other molecules such as protons (26)

and inositol triphosphate (18) that have been suggested as chemical mediators of transduction could be suggesting the need for a common element with which these suggested excitatory substances interact.

The cytoskeleton is such an attractive common element that could be influenced by all these chemical factors. In our model of photomechanical transduction, the ROS cytoskeleton is responsible for excitation, signal amplification and adaptation. The basis of this model is that a light-induced change in the structure of the discs and/or filaments leads to a change in the surface areas of the plasma membrane via the interconnecting filaments. The area of the plasma membrane effected by a single photon absorption obviously depends on the mechanical coupling properties of the filaments. Sensitivity control can be achieved if background illumination decreases intracellular mechanical coupling.

The steps in this mechanical coupling model are the following and are shown in Figure 2. A light induced conformational change in rhodopsin leads to a binding of G-protein to metarhodopsin II. This causes rapid ROS shrinkage which is experimentally observed by infrared light scattering. As a result of this shrinkage the plasma membrane area decreases, altering the structures of the channels and initiating the release of cyclic GMP together with the rising phase of the electrical response. Interestingly, such stress related channel have recently been isolated from chick skeletal muscle, and it is known that mechano-receptors are ubiquitous in nature (27).

The latter phase of the electrical response is accounted for by the subsequent activation of guanylate cyclase and the phosphodiesterase by rhodopsin activated T-protein. The result of this is a relaeas of protons and these protons may alter the filament structure and change the binding of calcium and other chemicals. The ability of the filaments to act as a proton buffer would account for the obervation of only a small change in pH in response to illumination (28). In addition, alteration in the filament structure could induce further stress on the plasma membrane causing a graded maximal electrical response.

In this model the conformation of the filaments determines the extent of mechanical coupling and signal propogation within the cell. We postulate that the filaments in the dark exhibit maximal mechanical coupling. With light, the filament structure is altered reducing the mechanical coupling and similar photon intensities will not be able to elicit the same response. Possible regulation of the elasticity of these cytoskeleton filament proteins could involve calcium, inositol triphosphate,

phosporylation or dephosphorylation of the filaments or some combination of the above.

If indeed the rod cell is a photomechanical transducer, then it is not surprising that such behavior could escape detection. Other mechanical transducers such as hair cells and Pacinian corpuscles are well protected from extraneous mechanical stimuli. In order to test our hypothesis it will be important to carefully design experiments in which the mechanical stimulation of the rod outer segment closely mimics the intracellular stress produced by photon absorption. We are hopeful that our suggestion will initiate experiments to quantitatively assess the photomechanical properties of the rod cell. An example of such an experiment was recently performed on the invertebrate squid retina where mechanical movement originating in the outer segment layer was observed on the smae time scale as the electrical response and was adapted to backgroung light illumination in a similar fashion (29). In addition, as future experiments elucidate the chemical composition of the ROS cytoskeleton, it should be possible to use chemical mediators of all the cytoskeleton proteins to precisely delineate the role of the intracellular filaments in regulating the plasma membrane electrical properties.

In summary, our ability to develop such an integrated model of amplification and adaptation without the need for an excitatory second messanger should hopefully stimulate new ways to view visual transduction and sensitivity control.

2. Experiments based on this guiding framework

(i) Probing the photoreceptor cytoskeleton with specific drugs and reagents

To understand the fundamental interactions that govern the mechanical properties of photoreceptor cells we began to test various reagents that are known to effect cytoskeletal components in various cellular systems. Among these reagents were taxol, nocodazole, cytochalasin B and cytochalasin D. All of these readents were dissolved in dimethyl-sulfoxide (DMSO) to a final concentration which was mM. The total DMSO concentration applied to the cells never exceeded 0.4%. Even at this concentration however the DMSO did perturb the cells slightly. Nonetheless the effect of these reagents was quite dramatic and could readily be seen over the small DMSO perturbation.

The cells were viewed in these experiments with an IM 35 inverted microscope. In order to keep the cells in a fixed position during the addition of the reagents the slides, on which the cells were viewed, were first coated with positively charged

polylysine. This held the photoreceptors down to the slide as a result of the electrostatic interaction between the positive slide and the negative cell. Not only was such a proceedure important for the addition of the reagents but also in the washing out of these reagents which was accomplished by rinsing the cells in the same buffer but without the specific chemical. Photographs were taken before and after both the addition and washing out proceedures.

Nocodazole, which is known in other cellular systems to bind to tubulin and cause destabilization in microtubular assemblies, had a most interesting effect on photoreceptors. As seen in Figure 3a a group of three cells is seen in this picture. Only one of these three cells still has the inner segment attached. These type of cells with the inner segment attached are well-known from electrophysiological studies to respond like normal photoreceptor cells on an intact retina. The picture in Figure 3b was taken after the addition of nocodazole. As can be seen the cells without inner segments have been washed away because their membranes were not intact and thus lacked the extent of negative charge required for poly-lysine to act like an electrostatic anchor. The cell with the inner segment however now has a definite bend in the outer segment. This bend can be eliminated and the cell returns back to its normal state by simply washing out the nocodazole by the proceedure described above. However once a cell has been made to bend in this fashion it will always bend back in the same direction no matter how many additions of nocodazole and nocodazole free ringer is added. We are now investigating the microtubule structure in photoreceptors in order to relate quantitatively the bending of the photo-receoptor with the extent of nocodazole binding.

Whereas cytochalasin B had the least perturbation on photoreceptor structure, cytochalasin D had a considerable effect on the inner segment. This drug is known to alter actin structures and its effect on the inner segment is in agreement with our earlier results, under the previous contract, that indicated important concentrations of actin in the inner segment. As can be seen in the photographs in Figure 4a and b, which were taken before and after addition of cytochalasin D, the inner segment basically falls apart and elongates tremendously after treatment with this reagent. Twenty minutes elapsed between the addition of the drug and the photograph in Figure 4b and at this point the process was irreversible. However, upto 16 minutes after addition of the chemical the process was full reversible. Studies are presently underway to test the interactions that are essential to the reversibility of the above process.

Before describing the results with taxol let us return to

the point discussed above concerning the effect of DMSO as a reagent used to add such drugs to photoreceptors. The problem with DMSO is that this chemical also effects photoreceptor membranes and we were faced with trying to assess the effects of the drug in the presence of a perturbing reagent. Thus we were searching for a substance that would allow us to investigate cytoskeletal effects without the need for DMSO. Although taxol is not such a drug, taxol allows us to investigate the primary effects of taxol with another completely non-perturbing reagent. Taxol is known to stabilize microtubules and D_2O is another reagent that has the same effect as taxol but does not have DMSO added with a chemical that causes other non-specific alterations. Therefore we could perform a parallel study with taxol and D_2O and determine what additional factors the DMSO may add to the equation. In fact we discovered that taxol and D_2O had identical effects. We will describe the effects in terms of D_2O but for all intents and purposes similar statements could be made for taxol. The sequence of photoreceptor alterations induced by D_2O is seen in Figure 5a, b and c. Figure 5a is the photoreceptor cell in frog ringers. Figure 5b is a few seconds after addition of D_2O and as can be seen the cell appears to shrivel slightly. Subsequently (Figure 5c), the outer segment begins to elongate tremendously and after the surrounding ringers washes out the D_2O the cell returns to its normal configuration without any sign of distortion. We have made a videotape of this process which we sent to the Letterman Army Institute of Research for analysis on their imaging equipment and that work is in progress. Taxol behaves identically except for a slight perturbation of the membrane that remains from the DMSO that was used to add the taxol. D_2O can permeate through the membrane of the cell without the need for the DMSO to cause the membrane alterations required to allow the entry of taxol or the other drugs. In addition the effect of D_2O is on the outer segment where all the machinery for light sensitivity lies therefore its effects are most important. Finally, since there are no extraneous perturbations from the addition of D_2O the results of these experiments will be easiest to interpret.

In summary, the most interesting results that we have obtained from this series of experimental investigations allows us to conclude that the cytoskeleton elements that govern inner segment structure are based on actin but, in the outer segment, the photoreceptor structure and cytoskeleton is dominated by microtubule assembly. Thus structural and mechanical alterations in the outer segment appear to be governed by those components that effect either tubulin or effect the interactions of tubulin molecules to form microtubules. Further experiments will be performed during the coming contract years to verify these preliminary conclusions.

(ii) Are there elastic changes in photoreceptor cells with light?

The results described in the last section were aimed at trying to determine the fundamental cytoskeleton chemistry that underlies the structure of photoreceptors and the interactions within photoreceptors. In this section we ask the crucial question that focuses on whether there are elastic changes in photoreceptors that are coupled with the absorption of light. Specifically what we are interested in is not only a yes or no answer to the above question but hopefully also an image of the areas of elastic alterations in the photoreceptors. After considerable research into possible methods that would give answers to these questions and many false starts we hit on a technique that allows us to conclude that not only are there elastic changes in photoreceptors with light but, in addition, these changes are focused in the outer segment where transduction of light energy occurs.

The method of choice was a new form of microscopy called acoustic microscopy where an image is formed not with light or electron beams but with sound waves. Even though conventional acoustic microscopy does not have the superresolution capabilities that we will describe in the next section of this progress report it does have some unique capabilities that are essential for the questions we want to answer. The unique features of acoustic microscpy are two fold. First, the image generated by an acoustic microscope reflects the stiffness of the material being imaged. Second, acoustic microscopy has pronounced subsurface capabilities. In essence ultrasound penetrates optically opaque materials with a resolution that is comparable to optical microscopy. Furthermore, in addition to these generally unique features of acoustic microscopy there are also important advantages in the use of this form of microscopy to study photoreceptors. The most important of these advantages is the fact that acoustic waves do not excite the sample. Thus, we have focused on this feature and the abiltiy of acoustic waves to detect stiffness alterations in biological tissue.

The results of our research are summarized in Figures 6a and b. In Figure 6a we used a home-built reflection type scanning acoustic microscope designed for continuously tunable operation in the frequency range 0.8-2.0GHz. For this frequency range acoustic lenses with a radius of curvature of 0.00004m and an opening angle of 100 degrees are used. For our experiments we used oa frequency of 0.97GHz where our resolution was 1 micron. In Figure 6a we see a group of four toad photoreceptor outer segments. This acoustic image was formed without the cells being

exposed to any light. Figure 6b, however, was obtained without any change in the sample or the microscope except for the full illumination of the cells with visible light. As can be seen there are significant changes in contrast in the images of the outer segment. It is important to realize that contrast seen on acoustic images depends on the distribution of mechanical qualities of the object, namely its elasticity and viscosity. The underlying principle is absorption and reflection of high frequency sound waves by the components of the cells. The ultrasound signal is attenuated by the processes of absorption, through which sound is converted into heat, and of scattering, by which sound is redirected. The determinants of such absorption are related to the macromolecular species present. The determinants of scattering are related to variations in the overall mechanical properties of the sample. Our detection of contrast alterations in the outer segments with light is proof that light alters the mechanical characteristics of photoreceptor outer segments. Future experiments will be aimed at seeing how laser light effects these photoreceptor mechanical properties and at using the unique depth of field available in acoustic microscopy to investigate subsurface alterations with all forms of light.

Superresolution Near-field Scanning Optical Microscopy

In our previous contract with the Army we began the research that has led to a new form of microscopy called near-field scanning optical microscopy (NSOM). This new concept of superresolution microscopy, which can also be performed with acoustic waves, has the resolution of the best available scanning electron microscopes but requires no vacuum or the destructive characteristics associated with electron beams. With our present version of the microscope we are achieving better than 0.1nm vertical resolution and better than 20nm lateral resolution. In this section we will describe the most recent work that will allow us in the next contract period to form two dimensional images of photoreceptors under a variety of conditions without the fixation and other artifacts associated with electron microscopy.

What has allowed us to achieve such unique superresolution capabilities? Lateral resolution in conventional optical or for that matter acoustic microscopy is limited by diffraction effects. It has long been desireable to develop a non-destructive probe which can operate at atmospheric pressures with a spatial resolution approaching that of scanning electron microscopy. Such a probe would have applicability in diverse areas of science but it would be especially applicable to biological problems. Towards this goal we have developed NSOM to

provide spatial resolution far-exceeding that of diffraction limited systems while still using visible wavelengths (30-36). In this section we demonstrate that NSOM can even be used with very weak spectral phenomena and this bodes well for our study of photoreceptors with this unique form of microscopy. The spectral phenomenon we focus on in this section is fluorescence from a fluorophore with a quantum yield of <0.0004.

In NSOM, light transmitted through a submicron aperture in an opaque screen is used to form a light spot which is then scanned over an object to generate an image. If the aperture is in close proximity to the object to be resolved, i.e. within the near-field, then resolution is determined primarily by the size of the aperture rather than the wavelength. Quantitatively the near-field can be defined as the distance from the screen wherein the initially collimated radiation emanating from an aperture diverges by less than 20%. We have calculated this distance to be 1/10 the wavelength for an aperture that has a diameter of 1/10 the wavelength (37).

Therefore at optical wavelengths it is necessary to reduce vibrations to less than 20 nm to achieve the necessary positioning accuracy. Towards this end a 0.6m thick optical honeycomb table with an air mount vibration isolation system was used to eliminate vibrations above a few hertz.

Several different methods have been used in the past to fabricate the submicron apertures needed in near-field microscopy (30-36). However we have developed an inexpensive, rapid, and highly reproducible method for producing such apertures at the tips of metallized glass pipettes. Another advantage of this technique is that these highly tapered pipettes can probe recessed regions of rough surfaces. Apertures with diameters ranging from 50nm to 1000nm were formed from glass micropipettes using a two stage pulling process. The tip outer diameters were approximately 500nm for the smaller aperture pipettes. Indeed, tops with outer diameters of 20nm have been produced for use in microinjection of individual cells (38).

The pipettes were metallized with 8nm of chromium followed by 50nm of aluminum. The chromium was used as an adhesive layer between the glass pipette and the 50nm aluminum layer. Aluminum was chosen for its high absorption coefficient at optical wavelengths. Scanning electron micrographs of a 100nm diameter pipette and a 600nm diameter pipette are compared in Figure 7.

A schematic of the experimental apparatus is shown in Figure 8. Movement of the pipette was accomplished on a rough scale by micrometer driven stages. Fine positioning was achieved by

stacked piezoelectric transducers. The piezoelectric transducers were calibrated both interferometrically and microscopically. Light was passed through the pipette illuminating the aperture from below. The light transmitted by the aperture was then collected by a 25 power 0.55 numerical aperture (NA) microscope objective and focused on a SIT vidicon detector. Both the intensity of the light transmitted and the position of the pipette could be detected by this detector.

Due to the small distance through which the radiation is collimated after emanating from the aperture, it is necessary to know the vertical position of the pipette to within a few nanometers. Coarse vertical positioning was achieved by optically observing the pipette tip come into focus as it was moved toward the object. A small potential was placed between the pipette and the object to be scanned. The pipette was moved vetically upward in steps of 2nm until a tunneling current was measured at which time the pipette was within a few nanometers of the object surface. At this point intensity data was collected and the pipette was lowered and moved horizontally 25nm to the next postion.

The sample was illuminated through the pipette using a 100W tungsten lamp with a maximum intensity at 570nm for the transmission measurements. A dicroic mirror was used to cut of the shorter wavelengths. An argon ion laser in all lines visible mode was used for the fluorescence scans. A rotating sand blasted glass window was used to reduce the speckle noise of the laser. A cut off filter was placed between the microscope objective and the detector to block the laser light and to allow the far red emission to be transmitted to the detector.

Test patterns were made by contact printing a pattern from a mask formed by electron beam lithography (35,39). This mask of silicon nitride was placed in contact with a clear glass coverslip and the material to be deposited was then evaporated through the mask and onto the coverslip. For the transmission scans 50nm of chromium was evaporated whereas 50nm of 3,4,9,10-perylenetetracarboxylic dianhydride was used for the fluorescence measurements. The samples were then coated with 5nm of chromium to assure conductivity over the edge or grating. The patterns thus formed had sharp, well-characterized features as demonstrated by scanning electron microscopy, SEM. Such test patterns are essential to quantitatively assess the resolution of NSOM in both the transmission and fluorescence modes.

Figure 9 shows a transmission scan over a chromium step for both a 600nm and 100nm aperture. The distance from 12% to 88% transmission scales with aperture size. In Figure 10 the high

resolution NSOM data is compared to a linescan from an electron micrograph of the same edge. The SEM trace is a convolution of the edgeprofile with the beam profile and the secondary electron emission yield function. The edge profile can be estimated from the micrograph trace to have a width of 30nm assuming a beam diameter of 20nm. This finite width is a result of the contact printing process. The 12%-88% point in intensity of the NSOM trace is 60nm. This is the near-field beam profile convoluted with the 30nm edge width.

Using these results we can make quantitative comparisons between the SEM and both experimental and theoretical NSOM scans. The theoretical curve through the NSOM data in Figure 10 was generated by assuming exponential absorption in the chromium step and an intensity transmitted to the dtector scaling as the third power of the unoccluded area as suggested by Bethe (40). Also shown in Figure 10 is a conventional far-field optical line scan obtained from the edge using the same 0.55 NA objective lens as used for the NSOM scans. The solid line passing throgh these experimental points has been calculated from the theory for a conventional incoherent scanning optical microscope (40). The result of a similar calculation for a 1.4 NA objective is shown at the top of Figure 10. Thus, one can infer that resolution far exceeding the diffraction limit has been achieved using near-field scanning techniques.

Using the same 100nm pipettes as were used for the data above we have obtained scans of fluorescent edges and gratings. One such scan of a fluorescent grating of period 800nm is shown in Figure 11A. A densitometer trace of a scanning electron micrograph of the same perylene grating is also shown in Figure 11B. The sharpest maximum and minimum change in the fluorescence NSOM image is <50nm. Thus fluorescence NSOM grating scans have been demonstrated with resolution comparable to the aperture diameter used and an order of magnitude better than the emission wavelength.

Near-field scanning optical microscopy in both the transmission and fluorescence modes has been demonstrated. Resolution on the order of the aperture size has been demonstrated down to a scale of <50nm. The pipette type apertures provide a highly reproducible, easily fabricated and inexpensive type of submicron aperture. A two dimensional near-field scanning optical microscope with improved speed, positioning accuracy, vibration isolation and resolution has been completed within the past few weeks and experiments will be performed on this instrument during the coming contract years.

REFERENCES

1. Cohen,A.I. The Retina: Morphology, Function, and Clinical Characteristics (Straatsma, B.R. Hall, M.O. Allen, R.A., and Crescitelli, F., eds.) 31-62. (Univ. of California Press,) Berkeley and Los Angeles, 1969.)
2. Hagins, W.A. and Ruppel, H. Fred. Proc. 30. 64-68 (1971).
3. Roof, D.J. and Heuser, J.E. J. Cell Biol. 95, 487-500 (1982).
4. Usukura, J. and Yamada, E. Biomedical Res. 2, 177-183 (1981).
5. Del. Priore, L.V., Ph.D Thesis, Cornell University (Ithaca, NY, 1984).
6. Del Priore,L.V. and Lewis, A. Biophys. J. 47, 103a (1985).
7. Kuhn, H. Prog, Retinal Res. 3, 123-156 (1984).
8. Vuong, T.M., Worcester, D.L. , Pfister, C. and Chabre, M. Biophys. J. 47, 37a (1985).
9. Chabre, M. Cavaggopmo. A. Biochim. Biophs. Acta 382, 336-343 (1975).
10. Yee, R. and Liebman, P.A. J. Biol. Chem. 253, 8902-8909 (19
11. Kilbride, P. and Ebrey, T.G. J. Gen. Physiol. 74, 415-426 (1979).
12. Heyman, R. Ames, A., Walseth, T., Barad, M., Graeff, R. and Goldberg, N. Biophys. J. 47, 101a (1985).
13. Goldberg, N.D., Ames, A. Gander, J.E., and Walseth, T.F., J. Biol. Chem. 258, 9213-9219 (1983).
14. Yoshikami, S., George, J.S. and Hagins, W.A. Nature 286, 395-398 (1980).
15. Gold, G.H. and Korenbrot, J.I. Proc. Natl. Acad. Sci. USA 77, 5557-5561 (1980).
16. Szuts. E/Z. Current Topics in Membranes and Transports (Miller, W.H., ed.) Vol. 15, 291-305 (Academic, New York, 1981).
17. George, J.S. Biophys. J. 41, 127a) (1983).
18. Waloga, G., Andersopn, R.E. and Irvine, R.F. Biophys. J. 47, 37a (1985).
19. Baylor, D.A., Lamb, T.D. and Yau, K. W. J. Physiol. 288 613-634 (1979).
20 Fain, G.L., J. Gen. Physiol. 261, 71-101 (1976).
21. Yau, K.W., Lamb, T.D. and McNaughton, M. Current Topics in Membranes and Transport (Miller, W.H., ed.) Vol. 15, 19-31 (Academic, New York, 1981).
22. Yau, K.W. and Nakatani, K. Nature 309, 352-354 (1985).
23. Fesenko, E.E., Kolesnikov, S.S. and Lyubarsky, A.L. Nature 310, 310-313 (1985).
24. Nakatani, K. and Yau, K.W. Biophys. J. 47, 356a (1985).
25. Cote, R.H., Birnbaum, M.S., Nicol, G.D. and Bownds, M.D. J. Biol. Chem. 254, 9635-9641 (1984).
26. Mueller, P. and Pugh, Jr., E.N., Proc. Natl. Acad. Sci. USA 80, 1892-1896 (1983).
27. Guharay, F. and Sachs, F.J. Physiol. (London) 352, 685-702

(1984).
28. Yoshikami, S. and Hagins, W.A. Biophys. J. 47, 101a (1985).
29. Yasaki, I. and Nakaye, T. Science 223, 411-413 (1984).
30. Lewis, A., Isaacson, M., Muray, A. and Harootunian, A., Biophys. J. 41, 405a (1983).
31. Lewis, A., Isaacson, M., Harootunian, A., and Muray, A., Ultramicroscopy 13, 227 (1984).
32. Pohl, D.W., Denk, W., and Lanz, M., Appl. Phys. Lett. 44, 652 (1984).
33. Fisher, U. Ch., J. Vac. Sci. Technol. B. 3, 1498 (1985).
34. Betzig, E., Lewis, A., Harootunian, A., Isaacson, M., and Kratschmer, E., Biophys. J. 49, 269 (1986).
35. Durig, U., Pohl, D. W., and Rohner, F., J. Appl. Phys. 59, 3318 (1986).
36. Betzig, E., Harootunian, A., Lewis, A., and Isaacson, M., Appl. Opt. 25, in press (1986).
37. Brown, K. T., and Flaming, D. G., Neuroscience 2, 813 (1977).
38. Kratschmer, E. and Isaacson, M., J. Vac. Sci. Technol. B. 4, 361 (1986).
39. Bethe, H. A., Phys. Rev. 66, 163 (1944).
40. Wilson, T., and Shepard, C., Theory and Practice of Scanning Optical Microscopy, (Academic Press Inc., London 1984), p.34

FIGURE CAPTIONS

Figure 1. Femtosecond Dephasing of Mudpuppy Cone Rhodopsin. Two measurements are shown to show the accuracy of the indirect femtosecond method.

Figure 2. A Mechanical Transduction Scheme
(a) Dark state of rod with dots on filaments representing chemical regulators of filament elasticity. In this configuration sodium channels are open with cyclic GMP bound and the filaments allow for maximal mechanical coupling.
(b) Light absorption by rhodopsin forming an intermediate, R*, capable of binding T-protein.
(c) T-protein binding to rhodopsin induces contraction of ROS which causes a decrease in area of the plasma membrane and initial release of cyclic GMP in a cooperative manner inducing the rising phase of the electrical response.
(d) Without necessarily changing cyclic GMP levels, protons and other chemical changes produced by phosphodiesterase activation alter the filament structure and elasticity by altering the chemical composition of the filaments. This is shown by a change of filament dots to filament squares. The change in filament structure puts further stress on the plasma membrane releasing more cyclic GMP and causing a maximal photoresponse. The change in filament elasticity locally adapts the cell in the region around the point of light absorption and photons with the same intensity produce less of a response in this adapted region.

Figure 3. (A) A Group of Cells before Addition of Nocodazole. Only the cell in the center of the field still has an inner segment and is physiologically active.
(B) The Field of View after Nocodazole addition. Only the cell with the inner segment has remained since it is electrostatically attached to the positive slide (see text). Notice the bend in the outer segment induced by Nocodazole.

Figure 4. (A) Photoreceptor Cell before Addition of Cytochalasin D.
(B) Photoreceptor Cell after Addition of Cytochalasin D.

Figure 5. (A) A Photoreceptor Cell in Frog's Ringers
(B) The Same Photoreceptor Cell a Few Seconds ater D2O Addition.
(C) The Same Cell with the Outer Segment Elongated

Figure 6. Acoustic Microscrographs of Photoreceptor Cells. (A) Before illumination with visible light

(B) After illumination with visible light

Figure 7. Scanning Electron Micrographs of Metallized Pipettes with Apertures of Diameters of 10nm and 50nm at the Tips of the Pipettes.

Figure 8. A Schematic of the Experiment.

Figure 9. Low Resolution (aperture=60nm) and High Resolution (aperture=10nm) Transmission NSOM Scans of a 50nm Chromium Edge are Shown Above. Wavelength used was 570nm.

Figure 10. NSOM and SEM Comparisons. From bottom to top are shown: a densitometer trace of a scanning electron micrograph of a 50nm thick chromium edge; an NSOM scan of the same edge use 570nm excitation plotted against a theoretical NSOM curve; a theoretical scanning optical microscope (SOM) scan, with 570nm excitation and NA=0.55, plotted with points from an experimental optical micrograph scan of the same 50nm thick chrome step taken with 570nm excitation and NA=0.55 collection optics used for the NSOM scans, and a theoretical SOM edge scan using a very high (1.4 NA) numerical aperture objective, 570nm excitation. All edge scan steps were normalized to an intensity change of unity.

Figure 11. A Fluorescent NSOM and SEM Comparison. A fluorescence NSOM scan of a perylene grating with a period of 800nm (A) is shown below a densitometer trace of a SEM scan of the same grating (B). The SEM scan was slightly displaced in a direction parallel to the grating lines relative to the NSOM scan.

Fig. 1

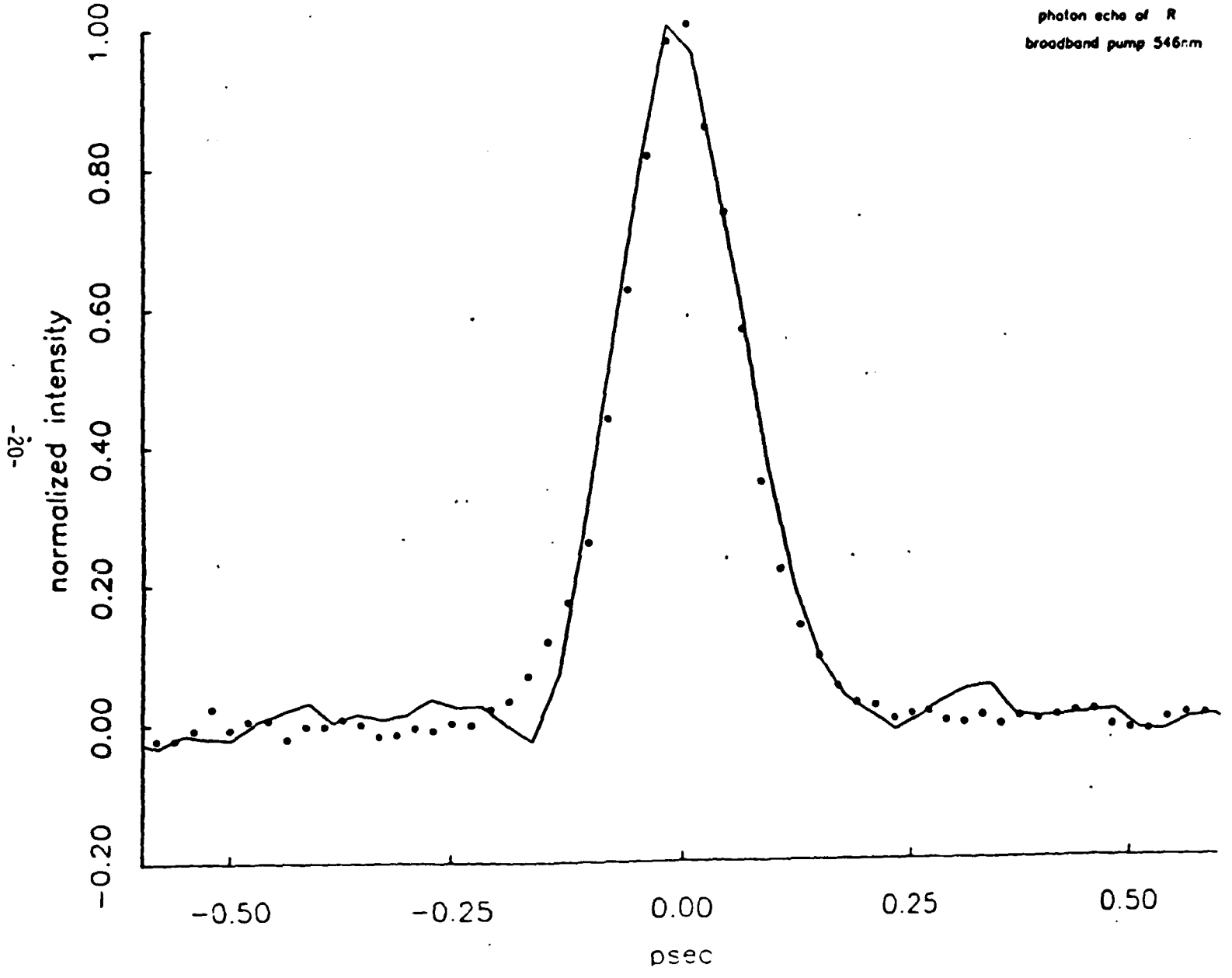
photon echo of R
broadband pump 546nm
normalized intensity
1.00
0.80
0.60
0.40
0.20
0.00
-0.20
-0.50
-0.25
0.00
0.25
0.50
psec

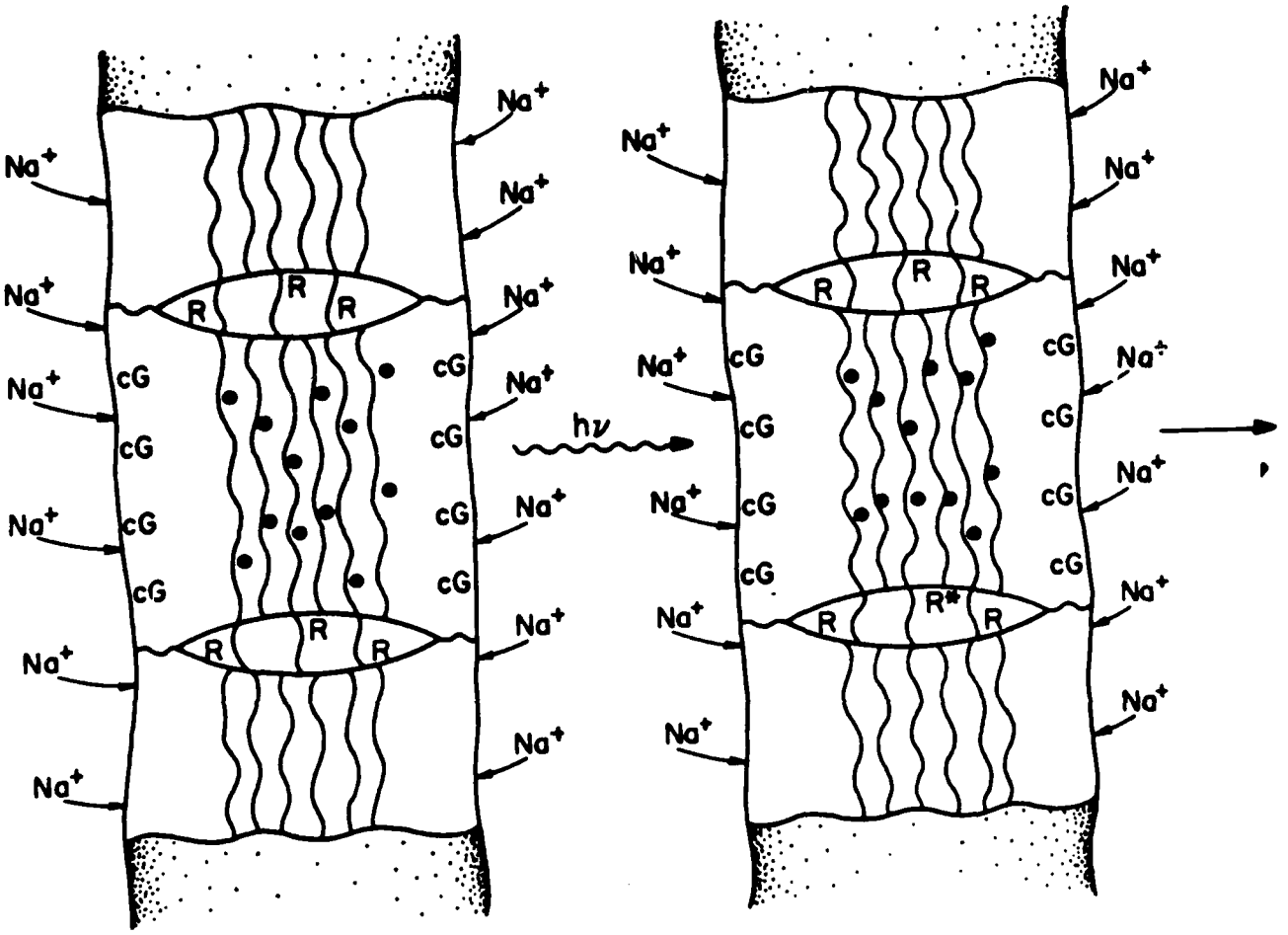

(a)
Fig. 2A

(b)
Fig. 2B

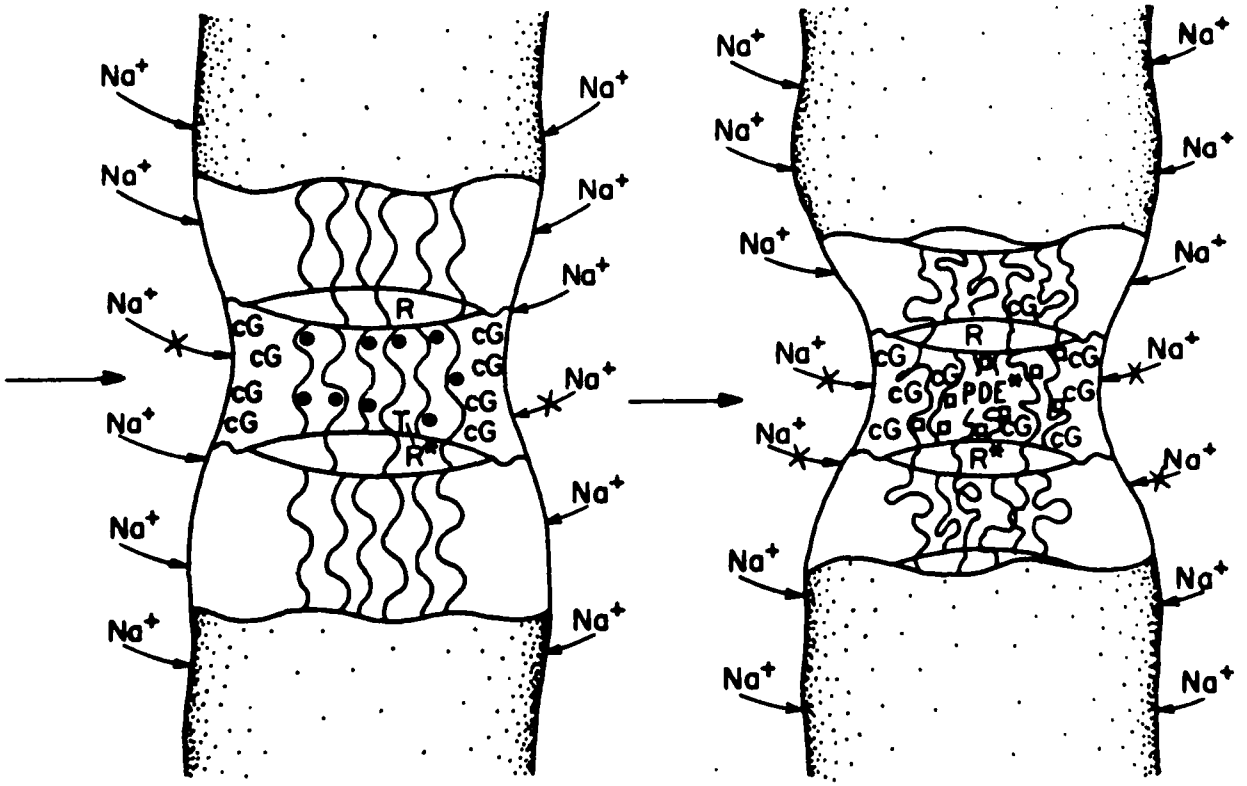

(c)

Fig. 2C

(d)

Fig. 2D

A

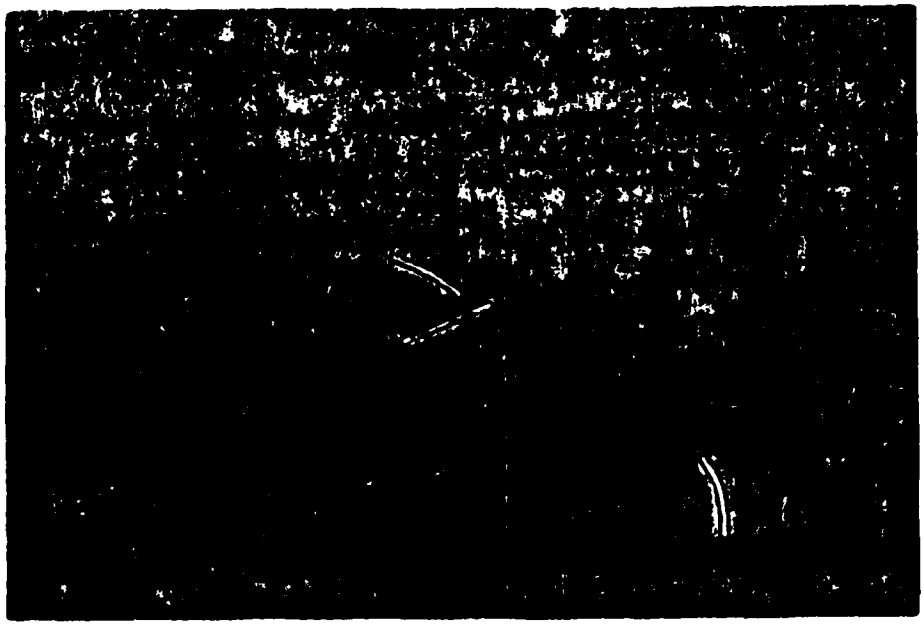

Fig. 3A

B

Fig. 3B

A

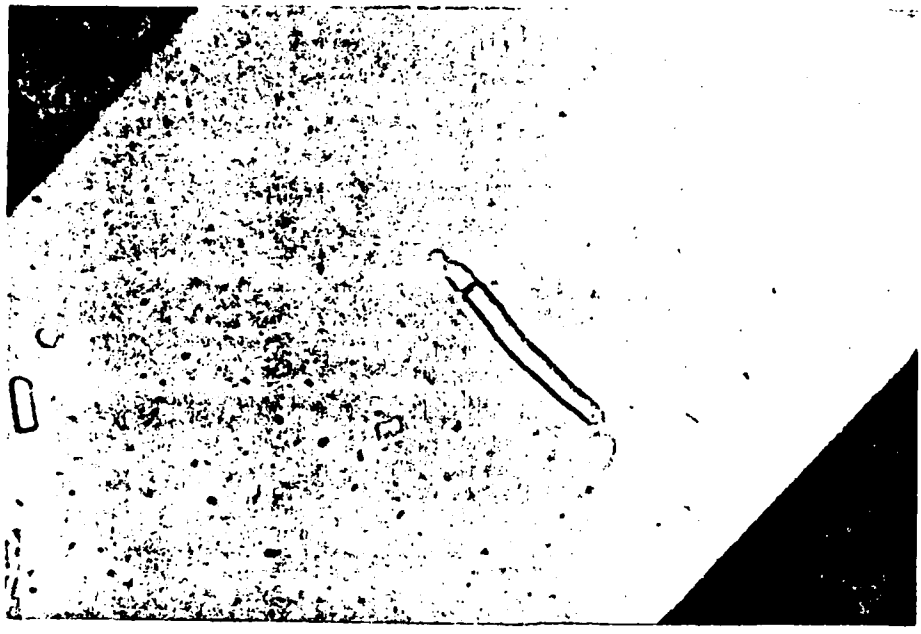

Fig. 4A :

B

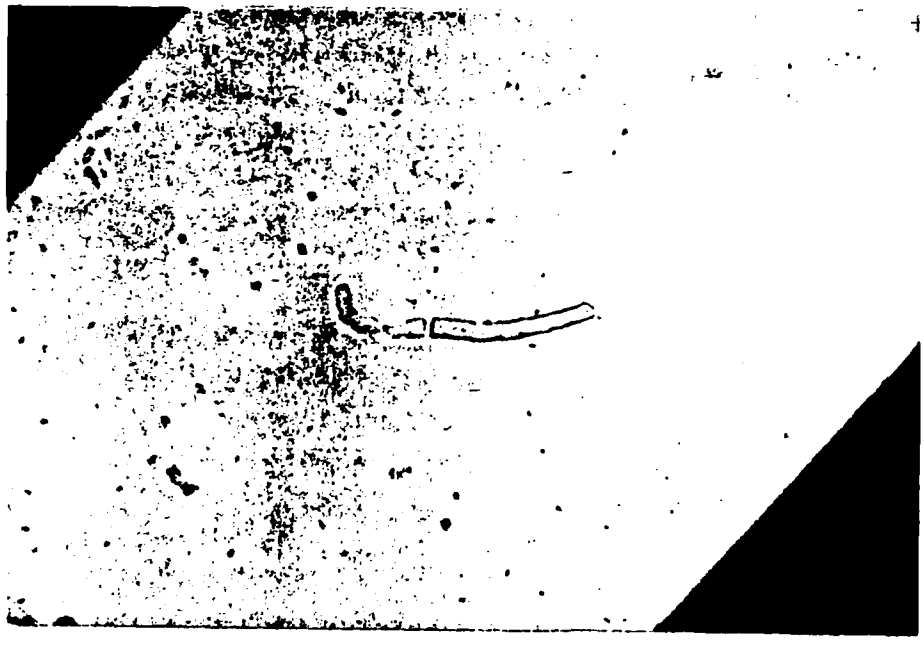

Fig. 4B

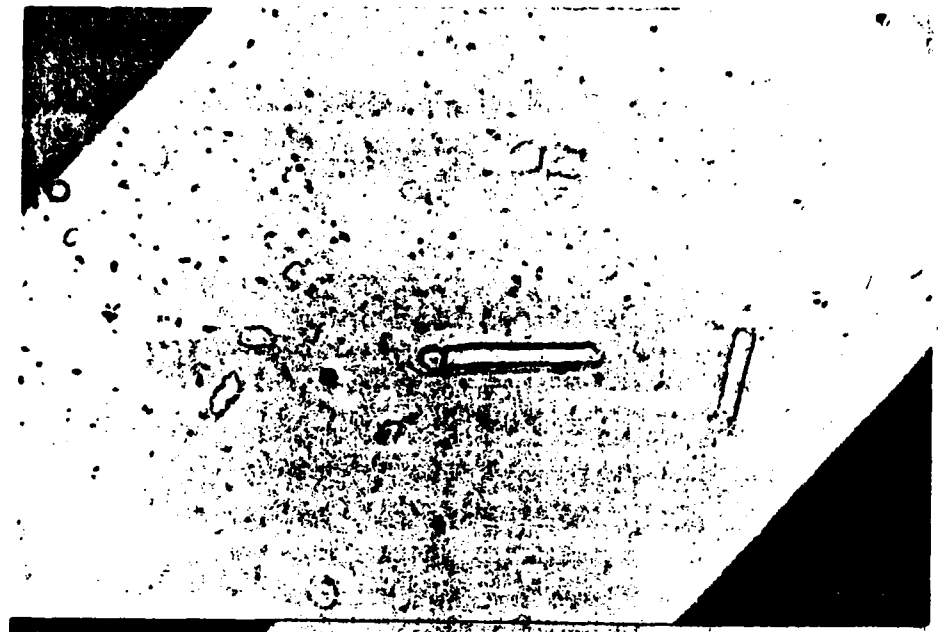

Fig. 5A

Fig. 5B

Fig. 5C

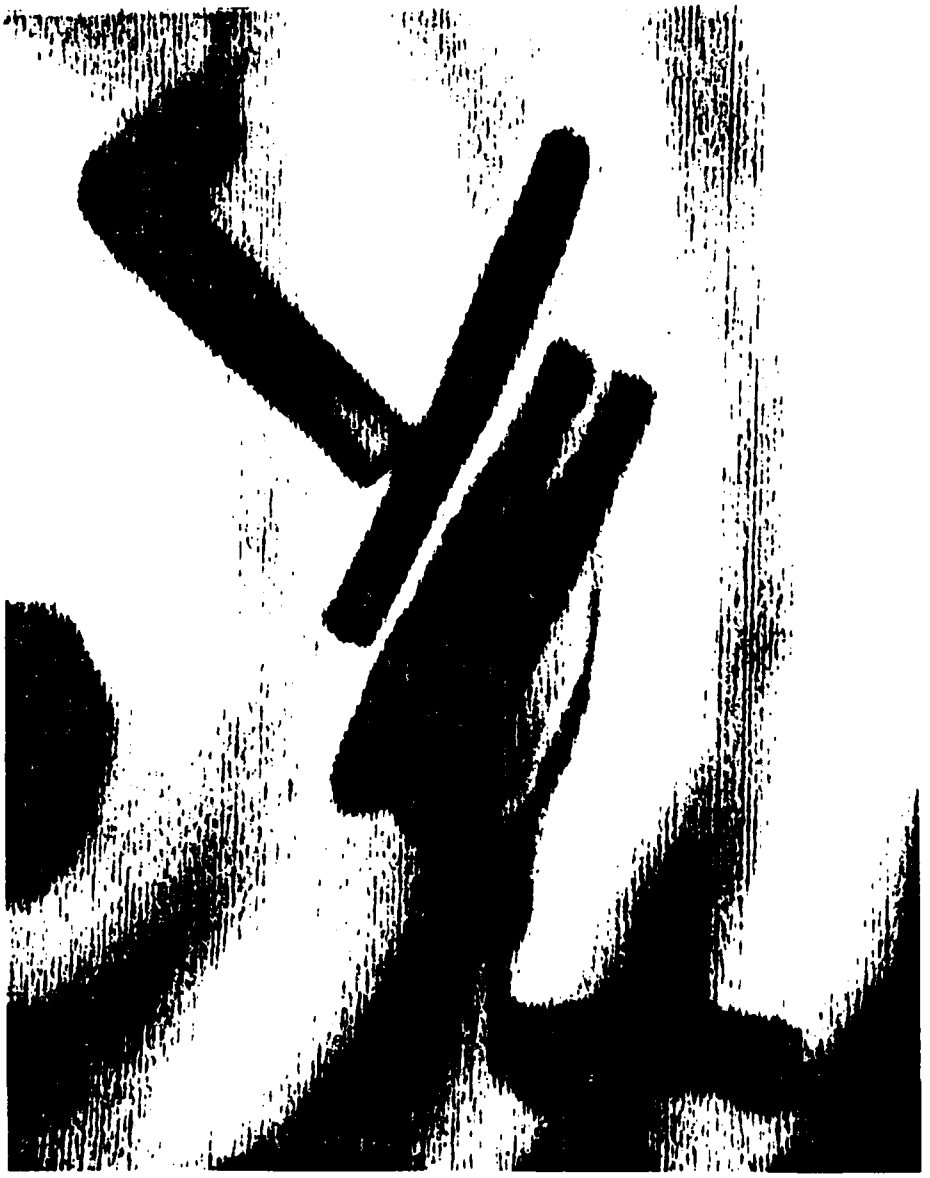

Fig. 6A

Fig. 6B

Fig. -

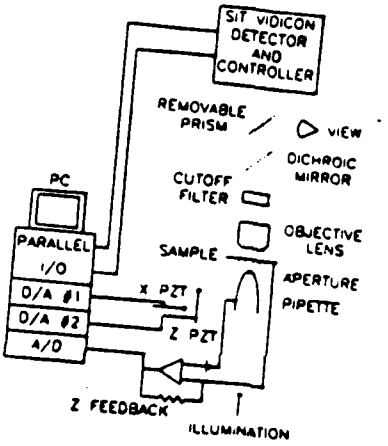
SIT VIDICON DETECTOR AND CONTROLLER
REMOVABLE PRISM
VIEW
DICHROIC MIRROR
CUTOFF FILTER
OBJECTIVE LENS
SAMPLE
APERTURE PIPETTE
PC
PARALLEL I/O
D/A #1
D/A #2
A/D
X PZT
Z PZT
Z FEEDBACK
ILLUMINATION

Fig. 8

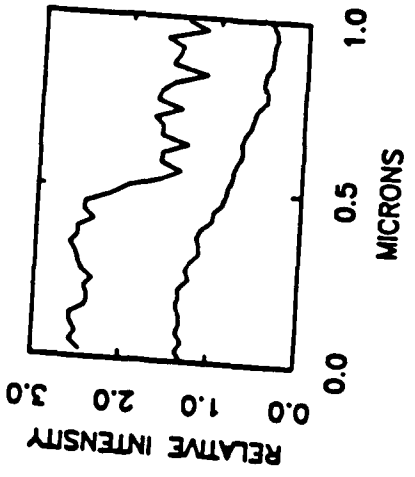

Fig. 9

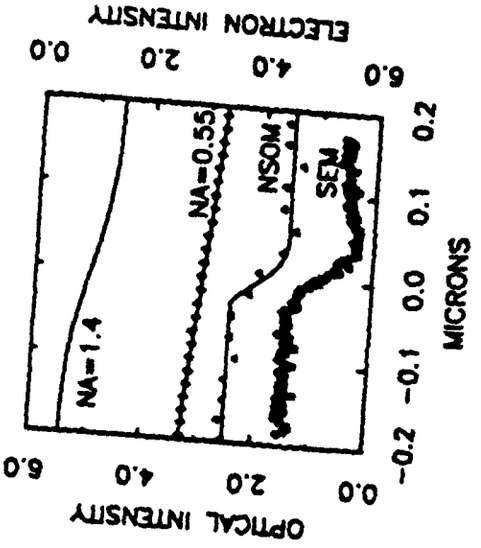
ELECTRON INTENSITY
0.0
2.0
4.0
6.0
NA=1.4
NA=0.55
NSOM
SEM
0.2
0.1
0.0
-0.1
-0.2
MICRONS
OPTICAL INTENSITY
0.0
2.0
4.0
6.0

Fig. 10

Fig. 11

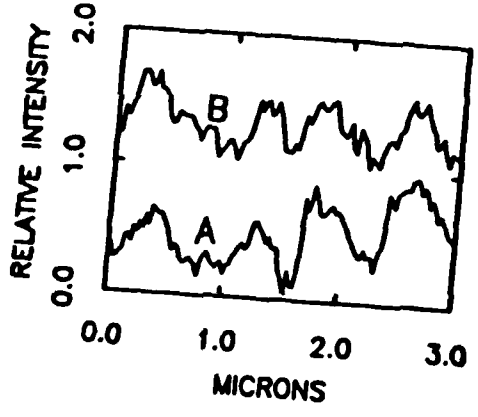

DISTRIBUTION LIST

4 copies	Commander Letterman Army Institute of Research (LAIR), Bldg. 1110 ATTN: SGRD-ULZ-RC Presidio of San Francisco, CA 94129-6615
1 copy	Commander US Army Medical Research and Development Command ATTN: SGRD-~~RMS~~ RMI-S Fort Detrick, Frederick, Maryland 21701-5012
2 copies	Defense Technical Information Center (DTIC) ATTN: DTIC-DDAC Cameron Station Alexandria, VA 22304-6145
1 copy	Dean School of Medicine Uniformed Services University of the Health Sciences 4301 Jones Bridge Road Bethesda, MD 20814-4799
1 copy	Commandant Academy of Health Sciences, US Army ATTN: AHS-CDM Fort Sam Houston, TX 78234-6100


DATE
FILMED
5-8